Junction Dynamics in Telechelic Hydrogen Bonded Polyisobutylene Networks

Marcus Müller,[†,‡] Alexander Dardin,[†,‡] Ulf Seidel,[†] Vittoria Balsamo,[†] Bela Iván,[§] Hans W. Spiess,[‡] and Reimund Stadler*[,†]

Institut für Organische Chemie, Becherweg 18-22, and Institut für Physikalische Chemie, Welderweg 11-15, Johannes Gutenberg-Universität, 55099 Mainz, Germany, and Max-Planck-Institut für Polymerforschung, Ackermannweg 10, 55128 Mainz, Germany

Received July 11, 1995; Revised Manuscript Received January 2, 1996[⊗]

ABSTRACT: 4-Urazoylbenzoic acid groups are attached to the chain ends of polyisobutylene. The cooperative assembling process of these polar groups is studied by DSC and dielectric and dynamic mechanical spectroscopy. The melting of the ordered clusters occurs in the temperature range 380−390 K. Distortions within the U4A clusters (Σ process) are monitored below the "melting" temperature T_m with dielectric spectroscopy. On a larger length scale, these distortions also lead to stress relaxation which can be probed by dynamic mechanical measurements. Near T_m, the relaxation of U4A multiplets (α* relaxation) is detected with dielectric spectroscopy. In this temperature range, dynamic mechanical measurements show a transition from elastic behavior to viscous flow. The results are rationalized with molecular modeling calculations.

1. Introduction

The presence of small amounts of polar or ionic groups attached to a nonpolar polymer chain has a profound effect on the systems' physical and rheological properties.[1−3] In telechelic end-assocating polymers, micelles are formed which consist of a cluster of attracting end groups and a corona of swollen chains.[4,5] The micelles are bridged by the flexible polymer chains. Such materials behave as reversible physical networks due to the finite lifetime of the clusters.

Semenov, Joanny, and Khokhlov[4] discussed possible stress relaxation paths in such systems. In their theoretical description, stress can be relaxed by a "creep motion" of the micelles, which requires either a deformation of micelles or a debridging of chains linked in a micelle.

In the case of telechelic ionomers, the dynamics of the ionic groups are described qualitatively by an "ion hopping" process.[2] However, this process is difficult to characterize on a molecular level. We have used in the past hydrogen bond complexation to analyze the static and dynamic properties of chains with few strong interacting sites. Besides simple binary interactions,[6,7] extended junction zones may be formed in such systems.[8−18]

Herein, telechelic polyisobutylene (M_n = 4800 g/mol) with one 4-urazoylbenzoic acid (U4A) unit at each chain end (PIB-U4A) (Figure 1) was synthesized and studied by DSC and dielectric and dynamic mechanical spectroscopy.

The structure of the hydrogen bonded assemblies formed by the urazoylbenzoic acid groups and the consequences of this assembling process on the mechanical properties has been studied in previous work. It was found that, in polybutadiene, functionalized statistically by U4A groups, linear associated chains are formed via acid−acid and urazole−urazole hydrogen bonded dimers[8,9] (Figure 1). At temperatures below 353 K, these linear associated chains assemble cooperatively to two-dimensional supramolecular clusters. According

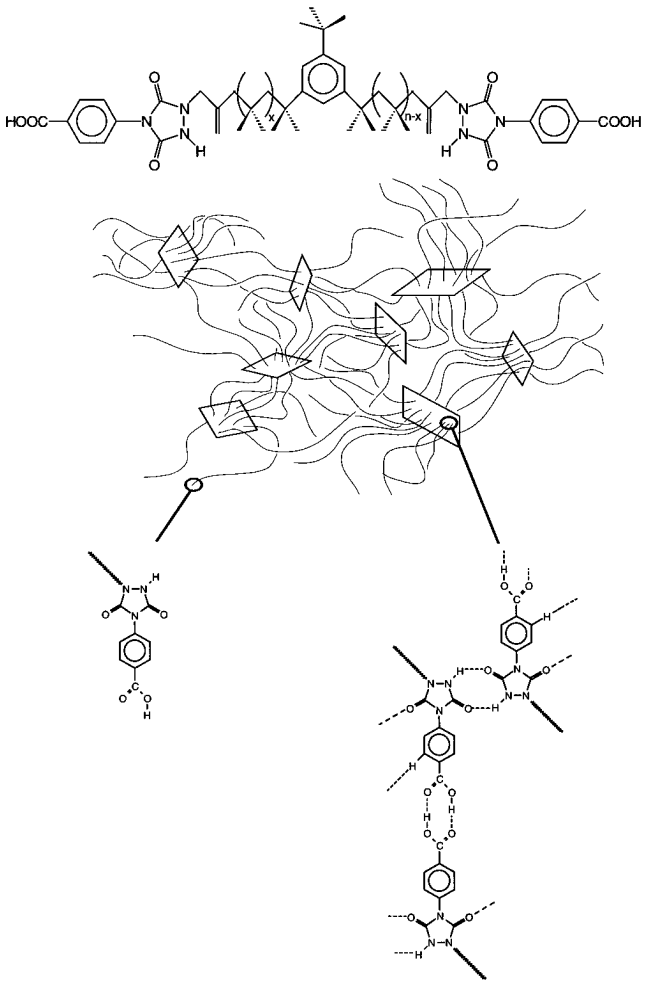

Figure 1. Hydrogen bonded telechelic polyisobutylene network. The 4-urazoylbenzoic acid groups form linear association chains via urazole−urazole and acid−acid hydrogen bonds. These association chains aggregate to supramolecularly ordered clusters (squares in the schematic representation).

* To whom correspondence should be addressed.
† Institut für Organische Chemie.
‡ Max-Planck-Institut für Polymerforschung.
§ Institut für Physikalische Chemie. Permanent address: Central Research Institute for Chemistry of the Hungarian Academy of Sciences, H-1525 Budapest, P.O. Box 17, Hungary.
⊗ Abstract published in *Advance ACS Abstracts,* March 1, 1996.

0024-9297/96/2229-2577$12.00/0

to the X-ray structure of a low molecular weight model compound, this cluster formation is due to hydrogen bonding between phenyl rings and urazole carbonyl groups.[10,11] The "melting" of supramolecularly ordered domains (first order transition) gives rise to an endotherm in DSC measurements.[12−14] Below this "melting" temperature, SAXS measurements show a scattering maximum which is due to the microphase separated supramolecularly ordered clusters in the amorphous polybutadiene matrix.[12,13] A characteristic absorption pattern in the carbonyl region of IR spectra is attributed to supramolecularly ordered clusters.[8,9]

The first investigations on the dynamics of the assemblies were done by ^{2}H-NMR spectroscopy on samples that were deuterated on the phenyl ring of each U4A group.[15,16] It was shown that the mobility of the phenyl rings is completely frozen as soon as these units are incorporated into supramolecularly ordered aggregates. Above the melting point of the clusters, all phenyl rings regain their full mobility.

Compared to randomly substituted polydienes, the use of telechelic polyisobutylene (Figure 1) has a variety of advantages and differences. In the case of randomly substituted polydienes, two "subchains" are attached to a functional group, whereas in telechelic polyisobutylene, only one chain is attached per functional unit. In the latter case the functional groups can pack more perfectly into the polar clusters. This enhanced packing is reflected by the higher melting temperature of clusters and by the formtion of macroscopic spherulites in the case of oligomeric isobutylene (M_n = 800 g/mol) with one U4A group at one chain end.[13,17,18] In addition, the spacing between two groups attached to the ends of a chain is given by the chain length. The main emphasis of the present work is the discussion of the cluster dynamics and the melting of the polar group assemblies based on dielectric experiments.

2. Experimental Section

Materials. Solvents (hexane, tetrahydrofuran (THF), and methylene chloride) were purified by conventional distillation procedures. Before use, isobutenyl (BASF) was passed through a drying column (Labclear gas filter; Aldrich) and then condensated under a dry nitrogen atmosphere. BCl_3 (1 M solution in CH_2Cl_2; Aldrich) and $TiCl_4$ (99.9%; Aldrich) were used as received. The initiator, 1,3-bis(2-hydroxy-2-propyl)-5-*tert*-butylbenzene, for living isobutylene polymerization was prepared as described elsewhere.[19a]

Synthesis of Isopropenyl-Telechelic Polyisobutylene. Isopropenyl-telechelic polyisobutylene (IPr-PIB-IPr) with $-CH_2C(CH_3)=CH_2$ termini at both chain ends was prepared by quantitative exospecific dehydrochlorination (with *t*BuOK in THF) of the corresponding *tert*-chlorine-telechelic PIB.[19b,c] PIB was synthesized by living cationic polymerization[19c] of isobutylene using a 1,3-bis(2-hydroxy-2-propyl)-5-*tert*-butylbenzene/BCl_3-TiCl_4 initiating system and a recently developed, simple laboratory procedure.[19d,e] After dehydrochlorination, the solution of IPr-PIB-IPr in hexane was chromatographed with a column filled with aluminum oxide (neutral, Brockman I; Aldrich) and molecular sieves (3 Å; Aldrich) to remove polar impurities. The solvent was removed by rotary evaporation, and the polymer was dried at 60 °C, under vacuum, to constant weight. The resulting isopropenyl-telechelic PIB was characterized by GPC (M_n = 4800, M_w/M_n = 1.13) and ^{1}H NMR for end-group functionality (F_n = 2.0).

Synthesis of PIB-U4A. The synthesis of the 4-urazoylbenzoic acid was performed according to the referenced literature description.[20] The functionalization of the polyisobutylene was performed analogous to the modification of polybutadienes.[20] The number of 4-urazoylbenzoic acid groups per chain is determined as 2.07 by ^{1}H-NMR. The degree of modification of the PIB-U4A is 2.3 mol % referred to the number of monomers.

Differential Scanning Calorimetry (DSC). DSC measurements were performed on a DSC7 (Perkin Elmer) with TAS7 software (Perkin Elmer). The instrument was calibrated using standard calibration procedures (indium). Before each measurement, the sample was heated to 423 K and cooled to room temperature at a cooling rate of 10 K/min. The measurements were performed at heating rates of 5, 10, 20, and 40 K/min. The sample weight was 7.2 mg.

Dielectric Spectroscopy. Dielectric spectroscopy was applied in a frequency range from $10^{-3}-10^7$ Hz. To cover the whole frequency range, two different measurement systems had to be employed: (a) a Solartron Schlumberger frequency response analyzer 1260, and (b) a Hewlett Packard impedance analyzer HP4192A. The sample was held between two gold plated capacitor plates with a diameter of 20 mm and a spacing of 0.05 mm. Temperature adjustment with a resolution of ±0.01 K was made by using a temperature-controlled nitrogen gas jet and a custom made cryostat.[21]

The generalized relaxation function proposed by Havriliak and Negami[22] was used for the quantitative data analysis:

$$\epsilon^*(\omega) = \epsilon_\infty + \frac{\Delta\epsilon}{(1 + (i\omega\tau)^\alpha)^\beta} \tag{1}$$

In this equation, α and β are parameters ($0 \le \alpha, \beta \le 1$) describing the symmetric and asymmetric broadening of the relaxation time distribution, τ is the mean relaxation time, and $\Delta\epsilon$ is the relaxation strength. The accuracy in the determination of the fit parameters α and β is ±0.05 and is ±10% in τ and $\Delta\epsilon$. An additional conductivity contribution in the dielectric loss spectra is fitted according to

$$\epsilon'' = \frac{\sigma}{\epsilon_0 \omega^s} \tag{2}$$

where σ and s are fit parameters and ϵ_0 denotes the vacuum permitivity.

Dynamic Mechanical Measurements. Dynamic mechanical measurements were carried out with a Rheometrics RDA2 in the oscillatory mode. To cover a broad temperature range, parallel plates with a diameter of 8 and 25 mm were used. The amplitudes were chosen to give the strongest possible force signal within the linear viscoelastic region. Measurements were performed in the frequency range of 0.0079−79.5 Hz with 6 measurements per decade. The temperature was varied between 213 and 343 K in steps of 10 K and between 343 and 393 K in steps of 5 K, respectively.

3. Results and Discussion

Molecular Modeling Calculations. Discussions of the self assembly of U4A groups in polymer matrices have been based on X-ray structures of model compounds.[10] Herein, we have performed semiempirical force field calculations to evaluate the tendency of cluster formation.

The linear association of chains formed by acid−acid and urazole−urazole hydrogen bonds is stabilized into a two-dimensional hydrogen bonded assembly by means of a "hydrogen bridge" between the phenyl ring and the carbonyl group C−H···O=C of a neighboring heterocycle. The calculated partial charge of the bonded aromatic hydrogen amounts to +0.23 compared to +0.16 of the nonbonded hydrogens, indicating the interaction of the bonded hydrogen with oxygen. These calculations support the interpretation of the X-ray data.[10] As can be seen by comparison of the structures in Figure 2 panels a and b, the supramolecular cluster formed by 16 U4A units resembles a layer of the *t*Bu-U4A single-crystal structure which was obtained from the X-ray analysis.[11]

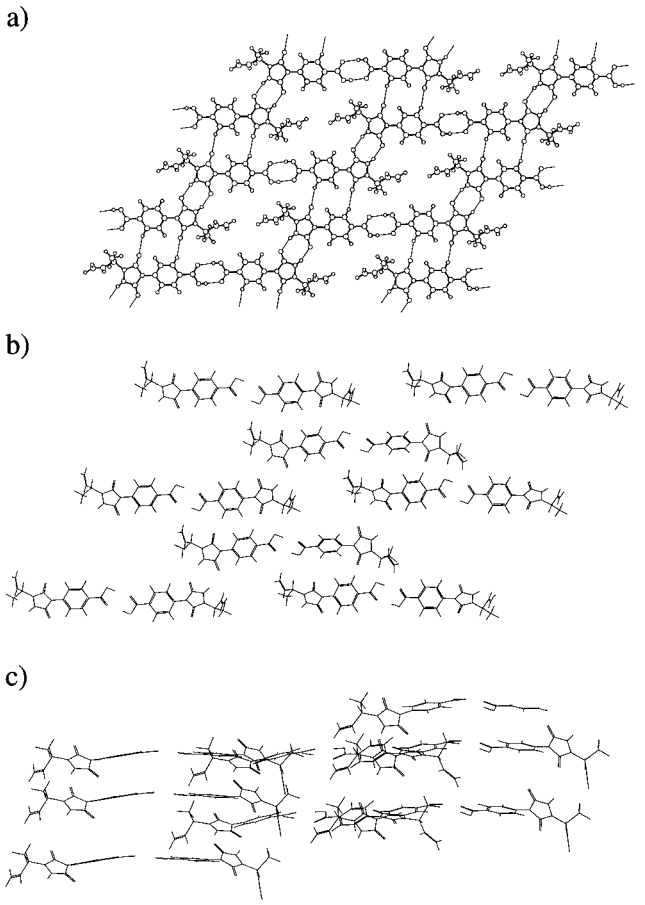

Figure 2. Comparison of the X-ray structure of *t*BU−U4A[10,11] (a) and the simulated structure (top (b) and side (c) views) of a U4A cluster.[15]

Table 1. Comparison of the Hydrogen Bond Distances and Torsion Angles As Obtained from the Energy Minimization and the Crystal Structure

	calcd	X-ray analysis[10]
distance −C═O--HO− (Å)	1.83−1.88	1.797
distance −C═O--HN═ (Å)	2.22−2.36	1.95
distance −C═O--HPh (Å)	2.1−2.77	2.25
torsion angle, urazole/ phenyl ring (deg)	34.7−42.6	39

The organization of the urazole units is not as perfect as in the crystal. Small deviations in the distances and slight distortions in the positions of the polar groups are the result of the energy minimization process rather than a homogeneous packing (Figure 2c). Nevertheless, in this two-dimensional array, the range of the hydrogen bond distances as well as the torsional angles between the heterocycle and the phenyl ring are in very good agreement with the values obtained from the crystal structure (Table 1).

These calculations indicate that hydrogen bond interactions between the polar groups are sufficient to explain the formation of a stable aggregate. The existence of a crystalline matrix is not required. Consequently, Figure 2 shows the view of the organization of the urazole units in a polymer matrix as two-dimensional assemblies.

The molecular dynamics within the supramolecular clusters, especially with respect to the mobility of the phenyl rings, is strongly affected by the third hydrogen bond. Figure 3 shows the rotational energies of a phenyl ring rotation for a single, free U4A unit and for a urazole unit within the hydrogen bonded assembly.

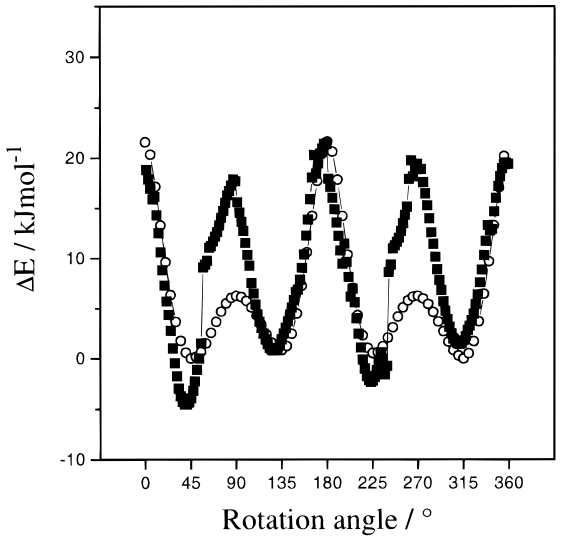

Figure 3. Calculated rotation energies of a phenyl ring rotation for a single, free U4A unit (○) in comparison with the energy barriers for a urazole unit within the hydrogen bonded assembly (■).

For the calculation of these rotational energies, the phenyl ring of one unit inside the minimized structure in Figure 2 was rotated, keeping the positions and conformations of the other units fixed. As can be seen from Figure 3, the presence of the phenyl carbonyl hydrogen bond has a strong impact on the rotation potential. For the free urazole unit, four minima at 39°, 127°, 232°, and 311° are obtained for a complete rotation of the phenyl ring. The barriers have a height of about 20 and 6 kJ mol^{-1}. These maxima correspond to the parallel and perpendicular orientation of the phenl ring plane with respect to the heterocycle. Phenyl rings inside the polar aggregates experience the additional hydrogen bond interactions with the carbonyl group of a neighboring heterocycle. This results in a rotational potential with only two absolute minima at 39° and 232°. The other two secondary minima exhibit an energy level which is higher by about 5 kJ mol^{-1} because in these positions the additional hydrogen bond is not active.

DSC Measurements. Figure 4 shows the DSC results for PIB-U4A with different heating rates: (a) 40 K/min, (b) 20 K/min, (c) 10 K/min, and (d) 5 K/min. All DSC traces show an endotherm, and the resulting peak maxima (T_m/K) are summarized in Table 2.

As has been shown in previous work,[12−14] this endotherm is related to the melting of supramolecularly ordered U4A clusters. The transition enthalpies (in ΔH/mol of [U4A]) are given in Table 2. The values are higher than those obtained for randomly functionalized polybutadiene with a comparable degree of modification (molecular weight $M_n = 10\,000$ g/mol).[13] The transition enthalpy is related to the number of functional groups which are incorporated into the supramolecular clusters. The high value of the transition enthalpy (average value $\Delta H = 15.0$ kJ/mol) in the case of telechelic polyisobutylene indicates that most (>95%) of the polar groups are incorporated into the U4A clusters.[13]

The fraction Φ of U4A units that are molten at a given temperature T_1 is obtained according to:

$$\Phi = \int_{T_0}^{T_1} \dot{Q}\, dT \Big/ \int_{T_0}^{\infty} \dot{Q}\, dT \qquad (3)$$

with $T_0 = 373$ K. Figure 4b (insert) shows the temper-

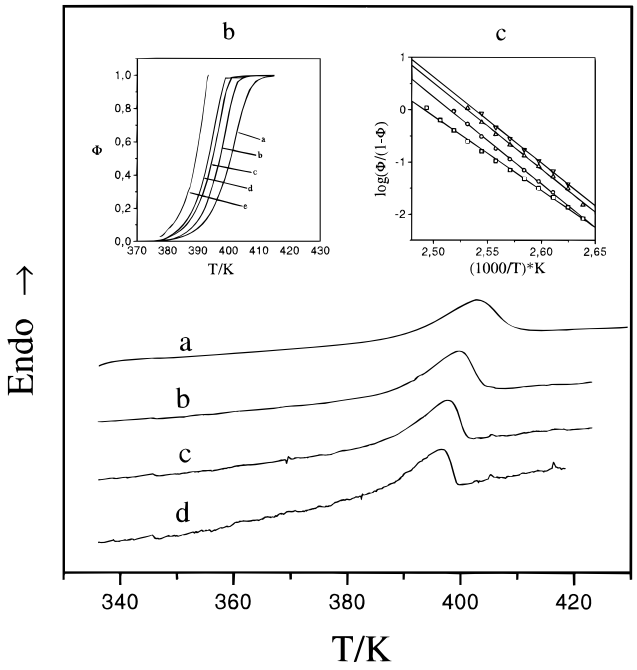

Figure 4. DSC heating traces of polyisobutylene, carrying one U4A group at each chain end (PIBU4A); heating rates: (a) 40 K/min, (b) 20 K/min, (c) 10 K/min, (d) and 5 K/min. The straight lines (insert b) correspond to the fraction of molten U4A groups (Φ) at the different heating rates a−d. From a−d, the corresponding Φ values at a heating rate of 0 K/min were extrapolated (e). Insert c shows $\ln(\Phi/(1-\Phi))$ as a function of inverse temperature 1/T for the different heating rates (□: 40 K/min, ○: 20 K/min, △: 10 K/min, ▽: 5 K/min).

Table 2. Melting Temperature T_m, Heat of Melting ΔH, and Cooperative Chain Length of U4A Clusters Obtained by DSC

	40 K/min (a)	20 K/min (b)	10 K/min (c)	5 K/min (d)
T_m (K)	402.6	399.8	397.5	396.6
ΔH [kJ (mol of U4A groups)$^{-1}$]^a	14.2	14.6	14.4	17.1
cooperative length	19	22	22	18

^{a} The mean value is 15.0 kJ mol^{-1}.

ature dependence of Φ as a function of temperature (T_1) for the different heating rates (a−d). Curve (e) is obtained by linear extrapolation of $\Phi(T)$ to (heating rate)$^{1/2}$ = 0 K/min to estimate the equilibrium and indicates that the clusters melt within a temperature range of 380−390 K. From the slope of $\ln(\Phi/1-\Phi)$ versus $1/T$ (Figure 4c), the activation enthalpy of melting is obtained. With the corresponding values of the heat of melting per U4A group a cooperative length of the clusters is calculated (Table 2).

Dielectric Spectroscopy. Dielectric loss spectra at two selected temperatures, one below the melting temperature T_m (T = 343 K) and one within the range of T_m (T = 394 K), are shown in Figure 5.

The spectrum at T = 343 K shows a maximum at a frequency of about 10^{-1} Hz. The further increase of the dielectric loss at frequencies smaller than 10^{-2} Hz is due to a conductivity contribution, which is taken into account by fitting it according to eq 2. The relaxation process, designated as Σ(structure) relaxation, is fitted by a Cole−Cole function[23] (i.e., β = 1 in eq 1) (dashed line in Figure 5). Even with a fit parameter β smaller than 1, it is impossible to obtain a good description of the data at the high frequency wing of this relaxation. To describe the data in this frequency range, a second

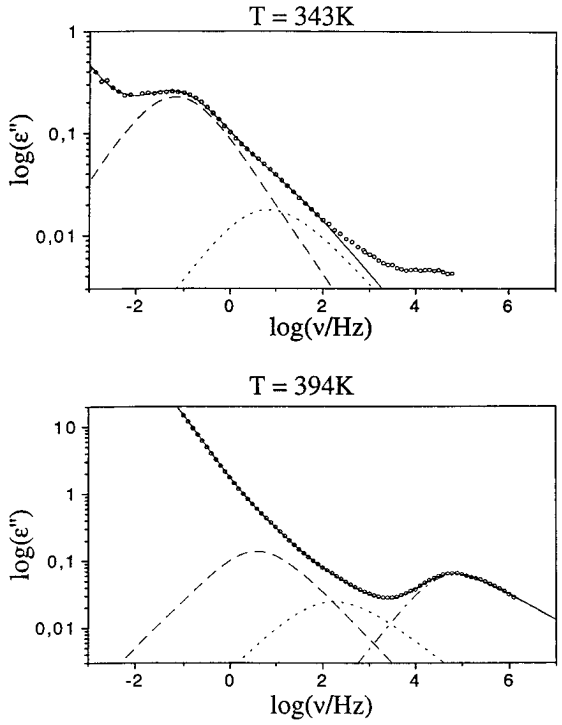

Figure 5. Dielectric loss curves of PIBU4A. The dashed line corresponds to the Σ relaxation, fitted with a Cole−Cole function;[23] the dotted line is an additional Havriliak−Negami fit;[22] which is necessary to describe the high frequency wing of the Σ relaxation; a second Havriliak−Negami function is used at 394.15 K for the α* relaxation (−•−); the solid line represents the sum of all fit functions.

Havriliak−Negami function must be used (dotted line). The relaxation strength of this function is about 16 times smaller than the relaxation strength of the Σ relaxation.

In the spectrum at T = 394 K, the Σ relaxation (dashed line) is shifted to higher frequencies. Additionally, a new relaxation maximum appears at a frequency of approximately 10^5 Hz (designated as α* relaxation). Though these two relaxations could be described by two Havriliak−Negami functions (i.e., $\beta \neq 1$ for both functions), a Cole−Cole function is used for the Σ relaxation to compare the results with the Cole−Cole fits at lower temperatures. Therefore, a third Havriliak−Negami function must be introduced to describe the experimental data. This additional Havriliak−Negami function is considered as the high frequency wing of the Σ relaxation and will not be discussed as a separate relaxation process.

In Figure 6, the α* relaxation is shown in the temperature range where the DSC endotherm is observed. At 382 K, the onset of the DSC endotherm, only a very weak α* relaxation is observed. The relaxation strength increases with increasing temperature.

In Figure 7, the relaxation strength of the α* and Σ relaxations are plotted with respect to temperature. The relaxation strength of the α* relaxation increases up to a temperature of about 393 K and then remains constant. The relaxation strength of the Σ relaxation behaves oppositively. It shows a strong decrease with temperature. The maximum value of the relaxation strength of the Σ relaxation is more than 4 times higher than that of the α* relaxation. The corresponding values of the third Havriliak−Negami function range between 0.05 and 0.1 independent of temperature.

From the frequency $2\pi\nu_{max}$ at maximum loss of the relaxation processes ϵ_{max}, the relaxation times τ_{max} =

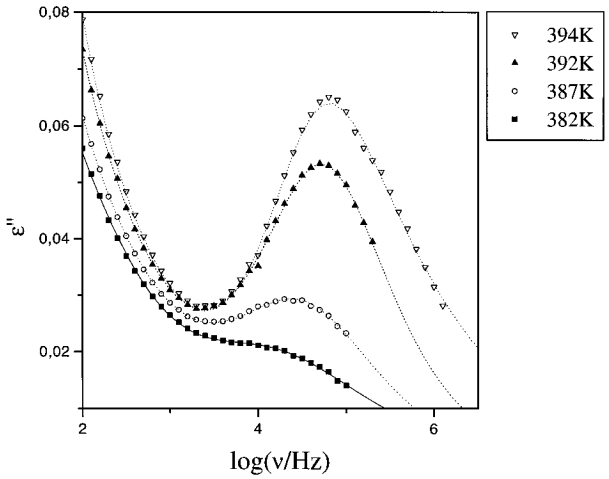

Figure 6. Dielectric α* relaxation of PIB−U4A at four selected temperatures.

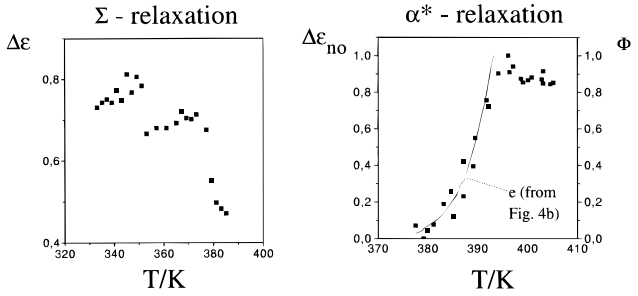

Figure 7. Temperature dependence of dielectric strength $\Delta\epsilon = \epsilon_s - \epsilon_\infty$ of the α* and Σ relaxation. The straight line is the fraction of molten U4A units, obtained from DSC (zero heating rate, e).

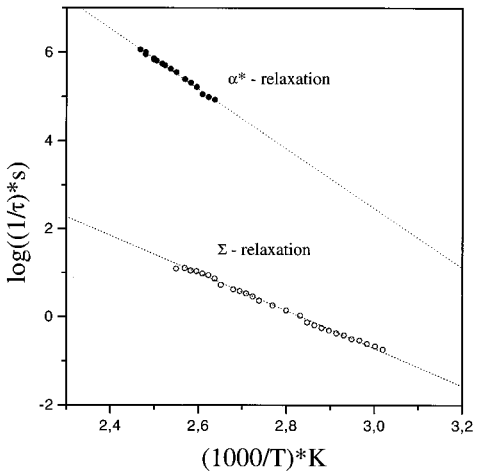

Figure 8. Temperature dependence of the relaxation time of the α* and Σ relaxation for PIB-U4A. The dotted lines are fit curves according to an Arrhenius law.

Table 3. Activation Enthalpy Δ*H* and Frequency Factor *A* of the Σ and α* Relaxation

	Σ relaxation	α* relaxation
ΔH (kJ mol^{-1})	78.3	129.7
A (Hz)	4.1×10^{11}	6.2×10^{22}

$1/2\pi\nu_{max}$ can be obtained. These relaxation times corresponding to the Σ and α* relaxation are shown as a function of T^{-1} in Figure 8.

The relaxation times of both processes show Arrhenius behavior. All parameters are given in Table 3.

In order to assign molecular motions to the different relaxation processes, the temperature dependence of relaxation time and strength have to be considered. The α* relaxation is detectable at the temperature where the onset of the melting endotherm is observed in the DSC. The normalized dielectric relaxation strength $\Delta\epsilon - \Delta\epsilon_{min}/(\Delta\epsilon_{max} - \Delta\epsilon_{min})$ of the α* relaxation and the fraction of molten U4A units obtained from DSC after extrapolation to zero heating rate (straight line (e), Figure 7) show a very similar temperature dependence. Obviously, this relaxation process is related to the dynamics of dipoles that originate as soon as the ordered clusters start to disintegrate. With increasing temperature, the number of these dipoles and thus the relaxation strength increase up to the temperature where all clusters are molten according to DSC. As polyisobutylene is dielectrically inactive,[24] those U4A units not incorporated in ordered clusters above T_m must be responsible for the α* relaxation. The interpretation of the α* relaxation is based on previous work, where the dynamics of thermoreversible polybutadiene networks (based on hydrogen bonded 4-phenylurazole dimers) have been studied.[7,25,26] It has been shown that the dimers give rise to a dielectric relaxation (α^*_{DIMER}) at frequencies below the α relaxation (T_g). In that case, dielectric spectroscopy monitors contributions of two relaxation mechanisms for the urazole dimers: the reorientation of hydrogen bonded complexes (with $\tau_{complex}$) and the dissociation of complexes (with $\tau^{ch}_{complex}$). If both relaxation times are of the same order, the dielectric relaxation τ^*_{compex} is given by[26]

$$\tau^*_{complex} = \frac{\tau^{ch}_{complex}\tau_{complex}}{\tau^{ch}_{complex} + \tau_{complex}} \qquad (4)$$

Therefore, if $\tau_{complex} \gg \tau^{ch}_{complex}$, the overall relaxation time is given by the lifetime of complexes $\tau^{ch}_{complex}$, whereas if $\tau_{complex} \ll \tau^{ch}_{complex}$, the overall relaxation time is defined by the tumbling time of complexes $\tau_{complex}$.

Similar relaxations should be observable in the more complex urazoylbenzoic acid systems. Above the melting temperature of clusters T_m, the U4A units exist either as uncomplexed U4A units or as U4A associated chains (multiplets). Analogous to the phenylurazole substituted polybutadienes, free U4A groups should have an effect on the dynamic glass transition of the polyisobutylene matrix. According to dynamic mechanical and DSC measurements, the dynamic glass transition occurs at frequencies of about 1 Hz at 213 K (Figure 11). At this temperature, no relaxation is detected in dielectric measurements. This shows that, in contrast to randomly substituted polybutadienes, all U4A stickers are incorporated into ordered clusters at temperatures below T_m. If the relaxation time of the α* relaxation is compared to the relaxation time of dimeric phenylurazole complexes (α^*_{DIMER} relaxation),[25] it appears that the relaxation of the U4A multiplets is slowed down by 3 orders of magnitude. As was outlined above, two relaxation paths (reorientation and dissociation) contribute to the relaxation of hydrogen bonded complexes. In analogy to the results obtained for phenylurazole dimers, it can be assumed that the reorientation of U4A multiplets is coupled to the cooperative motion of the polymer matrix. This should be described by the WLF behavior. Therefore, it might be assumed from the Arrhenius behavior of the α* relaxation that the dissociation of U4A multiplets is responsible for this relaxation. However, the temperatures where the α* relaxation is detected (T > 380 K) are far above the glass

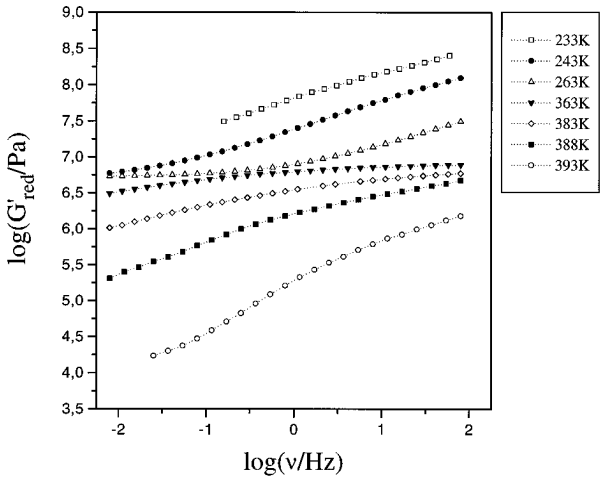

Figure 9. Storage modulus isotherms for seven selected temperatures.

transition temperature of polyisobutylene, and at such elevated temperatures ($T \gg T_g$), WLF behavior cannot be distinguished from Arrhenius behavior. The large activation energy of 129.7 kJ mol^{-1} and the high preexponential factor of 6.2×10^{22} Hz are unusual for Arrhenius behavior and therefore might reflect a cooperative motion of U4A multiplets. Whether the reorientation, the dissociation of disordered U4A multiplets, or both mechanisms are responsible for the α* relaxation remains unclear from the present results.

Below T_m, the only dipolar units are the ordered U4A clusters. Therefore, the Σ process must be related to a relaxation of these clusters. Two relaxation mechanisms may contribute[4] to the stress relaxation of end-associating polymers: the debridging of polymer chains and the deformation of micelles. The latter is designated as a breathing mode in the present case of two-dimensional assemblies, while the debridging process is associated with a dissociation of U4A groups from the U4A clusters. The possibility of relaxation via the debridging process can be excluded on the basis of 2D ^{2}H-exchange NMR experiments on low molecular weight model compounds selectively deuterated at the phenyl rings.[15] These measurements monitored well-defined slow 180° phenyl flips on a time scale of 100 ms up to 3 s at a temperature of 300 K. At this temperature, the dielectric Σ relaxation has a mean relaxation time of about 50 s (extrapolation of the data in Figure 8); i.e., both the well-defined phenyl flips and the dielectric relaxation are on the order of seconds. If the Σ relaxation resulted from a debridging process, the associated dissociation of the U4A complexes would lead to an isotropic motion of phenyl rings. Only if the urazole−urazole and acid−acid hydrogen bonds remain intact during the dielectric relaxation, can the well-defined "phenyl flips" which are actually observed in the exchange spectra be explained. Therefore, a debridging process cannot account for the dielectric Σ relaxation. On the other hand, a deformation of clusters should alter first the weak phenyl−carbonyl hydrogen bonds and, as a consequence, phenyl flips may occur. In addition, this deformation of clusters should also give rise to a large change in dipole moment which is in agreement with the high relaxation strength of the dielectric Σ relaxation. Thus, the overall dynamics of U4A clusters can be viewed as a deformation of the clusters in combination with well-defined phenyl flips occurring in the same time scale.

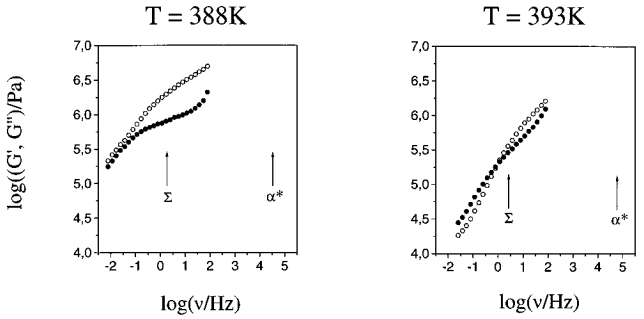

Figure 10. Storage (○) and loss (●) moduli at 388 and 393 K, respectively. The dielectric relaxation frequencies of the α* and Σ relaxation at the same temperatures are indicated by arrows.

Dynamic Mechanical Spectroscopy. Figure 9 shows the storage modulus isotherms obtained in the dynamic mechanical measurement. From the isotherms shown in Figure 9, it is not possible to construct a master curve. The material behaves thermorheologically complex.

At low temperature ($T < 263$ K), the upturn from the rubbery plateau to the glassy state is observed at high frequencies. The curves at high temperatures ($T > 363$ K) correspond to the transition from the rubbery plateau regime to viscous flow. Between 263 and 363 K the modulus shows a very small temperature and frequency dependence. At 393 K, the slope d log(G'/Pa)/d log ω is 0.61 within the low frequency regime. At higher temperature the force signal dropped to values too small to give reliable data.

In Figure 10, two sets of G' and G'' isotherms are shown for 388 and 393 K. At 388 K, G' still exceeds G'' in the entire frequency range, whereas at 393 K, a crossover of the G' and G'' values is observed. This indicates the transition from elastic behavior ($G' > G''$) to viscous behavior ($G' < G''$) at the temperature where the melting of the U4A clusters is observed in DSC.

Thus far, G' and G'' have been discussed at temperatures below and at the melting temperature T_m. Now let us consider the frequency dependence of G' and G'' at a fixed temperature near T_m (e.g., 388 K). As described in the work of Leibler, Rubinstein, and Colby,[27] the storage modulus G'' drops and a dispersion maximum in G'' is observed at $t = \tau$, as soon as the experimental time t ($t = 1/2\pi\nu$) exceeds the lifetime of the physical cross-links τ in thermoreversible networks. From the DSC experiment it can be deduced that, at 388 K, a fraction of the ordered U4A clusters has already transformed to more mobile and disordered U4A multiplets. Thus, two species act as physical cross-links in this temperature range: U4A multiplets and U4A clusters. Based on the theory of Leibler, Rubinstein, and Colby, two relaxation maxima should be observed for G''. At high frequencies (short experimental times t) stress can be relaxed as soon as t is larger than the lifetime of U4A multiplets. At lower frequencies (longer experimental times) further stress can be relaxed by the deformation of clusters or debridging processes as discussed above. If it is assumed that the G' curve is a superposition of two relaxation maxima, the maximum at low frequencies is at $\nu \approx 2$ Hz and the maximum at high frequencies occurs at values larger than 100 Hz. The relaxation frequencies of the dielectric Σ and α* relaxation are 1.7 and 3.2×10^4 Hz, respectively (indicated by arrows in Figure 10). From McCrum, Read, and Williams,[28] the correlation between the relaxation times obtained as the inverse frequency of

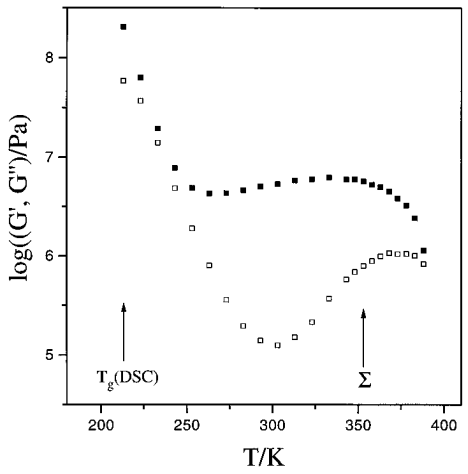

Figure 11. Temperature dependence of the storage (■) and loss (□) moduli at a frequency $\nu = 0.16$ Hz. At 353 K the dielectric Σ relaxation has the same relaxation frequency.

the loss modulus (τ_{DMA}) and the dielectric loss (τ_{DS}) is given by

$$\tau_{DS} = \frac{\epsilon_s}{\epsilon_\infty} \tau_{DMA} \quad (5)$$

with ϵ_s and ϵ_∞ being the values of the real part of the complex dielectric function at low and high frequencies, respectively. For both the Σ relaxation ($\epsilon_s = 2.8$ and $\epsilon_\infty = 2.3$, $T = 388$ K) and the α* relaxation ($\epsilon_s = 2.25$ and $\epsilon_2 = 2.17$, $T = 388$ K), the factor $\epsilon_s/\epsilon_\infty$ is close to 1. Therefore, the relaxation times of both methods can be compared directly.

The similar relaxation frequencies of the dielectric Σ relaxation and the corresponding relaxation in dynamic mechanical measurements can possibly be explained by distortions of the ordered clusters. The lower relaxation frequency in dynamic mechanical measurements may be due to a difference in length scale of distortions which are monitored. While dielectric relaxation probes fairly localized deformations, stress relaxation in dynamic mechanical spectroscopy may be sensitive to relaxations on a larger length scale with a lower relaxation frequency. The upturn of the G'' values at high frequencies may be due to the relaxation of U4A multiplets, which is also monitored in the dielectric α* relaxation.

In Figure 11, the temperature dependence of G' and G'' at a fixed frequency $\nu = 0.16$ Hz ($\omega = 1$ rad/s) is shown. The glass transition temperature T_g (=213.4 K) of the PIB chain measured by DSC is indicated. At temperatures between 250 and 350 K, G' increases slightly with temperature with a plateau of $G_P \approx 6$ MPa. Above 350 K, the storage modulus begins to drop and a broad dispersion maximum is observed in G'' at about 370 K. The temperature at which the maximum frequency of the dielectric Σ relaxation is 0.16 Hz is 353 K (arrow in Figure 11). As indicated above, both relaxations may be assigned to the distortion of U4A clusters.

4. Conclusions

In telechelic hydrogen bonded polyisobutylene, extended two-dimensional ordered U4A clusters are formed which break into U4A associated chains (multiplets) in the temperature range of 380−390 K. Below the melting temperature, distortions within the clusters are detected by dielectric spectroscopy (Σ relaxation or breathing mode). These distortions lead to stress relaxation in dynamic mechanical measurements similar to the prediction by Semenov et al. Near T_m, the onset of a second dielectric relaxation is detected at high frequencies. This process is assigned to either reorientation and/or dissociation dynamics of disordered U4A groups. In dynamic mechanical measurements, the transition from elastic behavior to viscous flow is observed in the same temperature range.

Acknowledgment. Financial support to this work by the German Israeli Foundation GIF, the Deutsche Kautschukgesellschaft, and the DFG through SFB 261 is gratefully acknowledged. M.M. and U.S. acknowledge the receipt of a stipend of the "Fond der Chemischen Industrie", and B.I. is grateful for an Alexander v. Humboldt Fellowship.

References and Notes

(1) Wilson, A. D.; Prosser, H. J. *Developments in Ionic Polymers 1*, Applied Science Publishers, Oxford, England, 1983.
(2) Eisenberg, A.; King, M. *Ion Containing Polymers*, Academic Press, New York, 1977.
(3) MacKnight, W. J.; Earnest, T. R., Jr. *J. Polym. Sci. Macromol. Rev.* **1977**, *16*, 41.
(4) Semenov, A. N.; Joanny, J. F.; Khokhlov, A. R. *Macromolecules* **1995**, *28*, 1066.
(5) Bagrodia, S.; Wilkes, G. L.; Kennedy, J. P. *Polym. Eng. Sci.* **1986**, *26*, 662.
(6) Freitas, L. L.; Stadler, R. *Macromolecules* **1987**, *20*, 2478.
(7) Müller, M.; Seidel, U.; Stadler, R. *Polymer* **1995**, *36*, 3143.
(8) Abetz, V.; Hilger, C.; Stadler, R. *Makromol. Chem., Macromol. Symp.* **1991**, *52*, 131.
(9) Hilger, C.; Stadler, R. *Polymer* **1991**, *32*, 3244.
(10) Seidel, U.; Hilger, C.; Hellmann, J.; Schollmeyer, D.; Stadler, R. *Supramol. Sci.* **1995**, *2*, 45.
(11) Hilger, C.; Dräger, M.; Stadler, R. *Macromolecules* **1992**, *25*, 2498.
(12) Hilger, C.; Stadler, R. *Macromolecules* **1990**, *23*, 2095.
(13) Hilger, C.; Stadler, R. *Macromolecules* **1992**, *25*, 6670.
(14) Hilger, C.; Stadler, R. *Makromol. Chem.* **1991**, *192*, 805.
(15) Dardin, A.; Boeffel, C.; Spiess, H. W.; Stadler, R.; Samulski, E. T. *Acta Polym.* **1995**, *46*, 291.
(16) Dardin, A.; Stadler, R.; Boeffel, C.; Spiess, H. W. *Makromol. Chem.* **1993**, *194*, 3467.
(17) Schirle, M. Doctoral Dissertation, Universität Mainz, 1994.
(18) Schirle, M.; Hoffmann, I.; Pieper, Th.; Kilian, H. G.; Stadler, R. *Polym. Bull.* **1996**, *36*, 95.
(19) (a) Wang, B.; Mishra, M. K.; Kennedy, J. P. *Polym. Bull.* **1987**, *17*, 205. (b) Kennedy, J. P.; Chang, V. S. C.; Smith, R. A.; Iván, B. *Polym. Bull.* **1979**, *1*, 575. (c) Kennedy, J. P.; Iván, B. *Designed Polymers by Carbocationic Macromolecular Engineering: Theory and Practice*; Hanser Publishers: Munich and New York, 1992; pp 168−178. (d) Everland, H.; Kops, J.; Nielsen, A.; Iván, B. *Polym. Bull.* **1993**, *31*, 159. (e) Feldthusen, J.; Iván, B.; Müller, A. H. E.; Kops, J. To be published.
(20) Hilger, C.; Stadler, R. *Makromol. Chem.* **1990**, *191*, 1347.
(21) Kremer, F.; Boese, D.; Meier, G.; Fischer, E. W. *Prog. Colloid Polym. Sci.* **1989**, *80*, 129.
(22) Havriliak, S.; Negami, S. *Polymer* **1967**, *8*, 161.
(23) Cole, K. S.; Cole, R. H. *J. Chem. Phys.* **1941**, *9*, 341.
(24) Rizos, A. K.; Jian, T.; Ngai, K. L. *Macromolecules* **1995**, *28*, 517.
(25) Müller, M.; Kremer, F.; Stadler, R.; Fischer, E. W.; Seidel, U. *Colloid Polym. Sci.* **1995**, *273*, 38.
(26) Müller, M.; Stadler, R.; Kremer, F.; Williams, G. *Macromolecules* **1995**, *28*, 6942.
(27) Leibler, L.; Rubinstein, M.; Colby, R. H. *Macromolecules* **1991**, *24*, 4701.
(28) McCrum, N. G.; Read, B. E.; Williams, G. *Anelastic and Dielectric Effects in Polymeric Solids*; Dover: New York, 1991; p 109.

MA950984Q